Model of precipitation and vertical air currents[1]

By EDWIN KESSLER, *National Severe Storms Laboratory, NOAA, Norman, Oklahoma, 73069, USA*

(Manuscript received February 15, 1973; revised version February 1, 1974)

ABSTRACT

Time-dependent moist columnar convection is numerically modeled; a version of Priestley's 1953 study of dry elements in a turbulent environment is combined with Kessler's 1969 treatment of the distribution of water substance in atmospheric circulations. Solutions are given of simultaneous equations for the vertical velocity, buoyancy, and cloud and precipitation content, in an air column moving under buoyancy and subject to rainout and continuous mixing of heat, momentum and moisture with ambient air. The velocity regime of the model depends on parameters of environmental lapse rate, moisture content, and the size and amplitude of an initiating disturbance. The model admits damped Brunt-Vaisala oscillations, condensation oscillations, and steady state updrafts of three kinds. Great changes of the solutions from one type to another occur as parameters cross thresholds determined by values of other parameters. Relationships among coupled periodic variations and steady state values of condensed water, precipitation rate, buoyancy and vertical velocity of air are analyzed in depth and with reference to microphysical processes. In the model, a definite horizontal size and perturbation buoyancy must be exceeded for sustained moist convection to accompany a given conditionally unstable lapse rate and ambient moisture condition. This leads to consideration of boundary-layer properties related to the geographical and diurnal variability of thunderstorms. It is proposed that strong static instability within the boundary layer tends to inhibit thunderstorm development because an unstable layer does not sustain large wave disturbances which may be essential to initiate deep convection and because the small scale convection promoted by strong boundary layer instability dissipates some of the energy that would otherwise remain available for deep convection. A number of other storm characteristics find plausible explanations within the framework of the theory, and some studies are suggested for its evaluation and improvement.

1. Introduction

This study of a model of atmospheric moist convection presents an appreciation of essential working relationships among important parameters and especially the role of buoyancy effects produced by water condensation, storage, and evaporation. We use much of Priestley's (1953) approach where the motion and temperature of a parcel of dry air driven by its own buoyancy is subject to the turbulent transfer of heat and momentum with an unchanging environment at rest. The three modes of motion Priestley derived depend largely on the scale of motion and not at all on the amplitude of an initiating disturbance. In our model of the conditionally unstable case, however, the amplitude of the initiating disturbance does strongly determine what follows. The remarkable natural phenomenology whose understanding we approach by numerical modeling has been lucidly discussed by Scorer and Ludlam (1953), and by Ludlam (1963), among others. Modeling problems as applied to moist convection have been thoughtfully and comprehensively reviewed and analyzed by Ogura (1972).

Our model uses continuity equations for water substance developed by Kessler (1969) with an equation, similar to one of Priestley's, that describes the variation of vertical air velocity in terms of thermal buoyancy, the load

[1] Developed version of a paper first presented at the International Meteorological Conference at Tel Aviv, Israel, Nov. 30–Dec. 4, 1970. Edited and abridged version of NSSL Technical Memorandum No. 54 (same title), by E. Kessler and W. C. Bumgarner, June 1971, 93 pp.

of condensation products, and entrainment of stationary environmental air. Another equation, analogous to a second of Priestley's, relates variations of thermal buoyancy to vertical velocity, to the lapse rate and moisture content of the environment, and to the heat transferred during either condensation or evaporation of cloud and precipitation.

Vertical averaging of water load and effective buoyancy in our model greatly simplifies the calculations while raising questions of rigor and applicability, but facilitates coverage of a great parameter space and the interpretation of working relationships whose authenticity can be tested against observations. Our analysis may also be viewed as an exploration of one common assumption of practicing forecasters, viz., that the intensity of convection is given in large part by the net positive area, enclosed on an adiabatic diagram by a surface parcel ascended to the tropopause, and its ambient sounding.

2. Modeling equations

The distribution of water substance in a vertical column is given by

$$\frac{\partial M}{\partial t} = -(V+w)\frac{\partial M}{\partial z} - M\frac{\partial V}{\partial z} + Mw\frac{\partial \ln \varrho}{\partial z} + \mathrm{AC} + \mathrm{CC} - \mathrm{EP} - k_5 M \qquad (1)$$

$$\frac{\partial m}{\partial t} = -w\frac{\partial m}{\partial z} + wG + mw\frac{\partial \ln \varrho}{\partial z} - \mathrm{AC} - \mathrm{CC} + \mathrm{EP} - k_5(m - m_0) \qquad (2)$$

Here M, always positive or zero, is the precipitation content of air; m when positive is the cloud content, and when negative is the saturation deficit; V, always a negative quantity, represents the terminal velocity of precipitation relative to the air; w is the vertical velocity of air, ϱ is the air density, and G is a condensation function. The terms on the right-hand side of the precipitation equation present, in order, the vertical advection of precipitation, an effect of the divergence of the precipitation fall speed, an effect of the compressibility of air, the spontaneous creation of precipitation from cloud (autoconversion, AC), the growth of precipitation by collection of cloud (CC), the evaporation of precipitation in dry air (EP),[1] and the depletion of cloud and precipitation through a mixing of cloudy air with environmental air whose saturation deficit is given by m_0. Details of the terms in eqs. (1) and (2) that account for microphysical processes are given in Table 1. Eqs. (1) and (2) define the distributions of vapor, cloud, and precipitation density when microphysical parameters and the vertical profile of the vertical air velocity are given. The derivation of these equations and the nature of their solutions have been discussed in depth by Kessler (1969).

The components of a model for the vertical velocity in 1-dimensional space have, so far, always involved several rather arbitrary features (Warner, 1970), partly because some important characteristics of cloud behavior are still not well understood, and because there is no proper basis for introducing the regulatory dynamic pressure without an explicit treatment of the columnar environment. In order to facilitate examination of working relationships between the water load and other parameters, our model is greatly simplified by constraining the vertical velocity profile to a parabolic shape, with the change of its magnitude with time affected by average values of thermal buoyancy and water load $\mathcal{L}$. The average thermal buoyancy may be identified in updrafts with the positive area on an adiabatic diagram, or in downdrafts with the negative area associated with the descent of evaporatively cooled air.

Thus, we treat not the growth of an isolated cloud tower as do Simpson & Wiggert (1969), nor do we allow the vertical velocity at each level in the troposphere to respond to the local buoyancy there as have Ogura & Takahashi (1971) in their less restrictive treatment. Instead we consider the development of a tropospheric condition with the vertical velocity given by

$$w = \frac{4w_{\max}}{H}\left(z - \frac{z^2}{H}\right) \qquad (3)$$

Eq. (3) is not wholly arbitrary, since air's real

[1] The term AC is applied only where m exceeds the autoconversion threshold a, usually 1 g/m³; the term CC is applied only where m is positive, i.e., where there is cloud; and the term EP is applied only where m is negative, i.e., where the air is not saturated (see Table 1).

Table 1. *Mathematical models of microphysical parameters*

Microphysical process or parameter	Mathematical representation
Condensation and evaporation of cloud (gm m^{-3} sec^{-1})	$wG = \frac{4w_{max}}{H}\left(z - \frac{z^2}{H}\right)(C_4 + C_5 z)$
Drop-size distribution parameter (m^{-4})	N_0
Autoconversion of cloud, AC (g m^{-3} sec^{-1})	$k_1(m-a)$ (for $m > a$ only)
Collection of cloud, CC	$k_2 E N_0^{0.125} m M^{0.875} \exp(k_7 z/2)$ (for $m > 0$ only)
Evaporation of precipitation EP (g m^{-3} sec^{-1})	$k_3 N_0^{0.35} m M^{0.65}$ (for $m < 0$ only)
Terminal velocity of precipitation (m sec^{-1})	$V = -38.8 N_0^{-0.125} M^{0.125} \exp(k_7 z/2)$

Main factors used in this study (m-g-s units):

$H = 10^4$	$N_0 = 10^7$	$k_1 = 10^{-4}$
$C_4 = 3 \times 10^{-3a}$	$a = 1$	$k_2 = 6.96 \times 10^{-4}$
$C_5 = -3 \times 10^{-7a}$	$E = 1$	$k_3 = 1.93 \times 10^{-6}$
		$k_7 = 10^{-4}$ $(k_7 = -\partial \ln \varrho / \partial z)$

[a] The choices of C_4 and C_5 correspond roughly to a summer or tropical atmosphere.

velocity must have an extremum between boundaries ($Z = 0, H$) where its velocity is zero.

In order to develop a velocity tendency equation reasonably consistent with (3), we consider the simplest case where a parcel starts from the lower boundary under the influence of constant buoyancy B:[1]

$$\frac{dw}{dt} = B \tag{4a}$$

As this parcel passes the level $H/2$, its velocity is $\sqrt{BH}$; subsequently effects of dynamic pressure and negative buoyancy implied by our choice of velocity profile, bring the parcel to rest. A chain of parcels originating at $z = 0$ have at each height, up to $H/2$, velocities that are close to those given by the lower half of the parabolic profile (2). This profile is created in a time $T = \sqrt{H/B}$, just the time required for a parcel to move from 0 to $H/2$ under the influence of buoyancy B, and once formed the profile is unchanging while the buoyancy is unchanging.

We seek the simplest equation that describes updraft development bounded by considerations of buoyancy and vertical advection and suggest

$$\frac{\partial \overline{w}}{\partial t} = B - \sqrt{\frac{B}{H}}\, w_{max} \tag{4b}$$

where $\overline{w}$ is the average updraft, the e-folding time is $\sqrt{H/B}$ and the steady maximum velocity is $\sqrt{BH}$ as desired. We recognize that effects of momentum exchange should be included, and the term $-k_5 \overline{w}$ is accordingly added on the right side of (4b). Then substitution of $2/3\ w_{max}$ for $\overline{w}$ leads to the equation

$$\frac{\partial w_{max}}{\partial t} = 1.5\left[B - \left|\frac{B}{H}\right|^{1/2} w_{max}\right] - k_5 w_{max} \tag{5}$$

where absolute value is taken inside the brackets in order to provide downdrafts with negative values of (now variable) B.[2]

The buoyancy has two components. The thermal component a may be positive or negative and is akin to the area enclosed on an adiabatic diagram by the intersections of a sounding in the environment and a sounding in the thermal column. The contribution of condensate to buoyancy is always negative and is proportional to the average density of cloud plus precipitation in the thermal column, as defined at each

[1] Alternate derivations of the buoyancy equation and of the buoyancy tendency equation are given in the appendix.

[2] As shown in the appendix, (5) is the linearized form of an equation rigorously derived. Although the nonlinear equation can be as readily integrated numerically, we utilized the linear equation during the study for purposes of comparison of certain numerical and analytic results. Subsequent comparison of the linear and nonlinear numerical models showed the differences to be small (about 10 % of representative vertical velocities, for example).

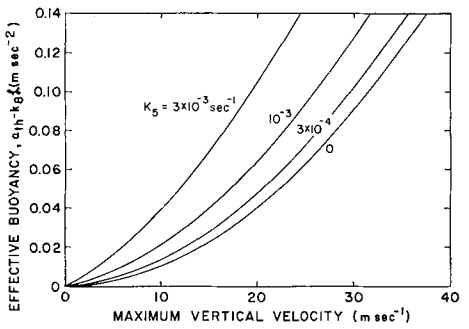

Fig. 1. Steady state maxima of vertical velocity in relation to effective buoyancy, defined by eq. (5), for several values of the momentum mixing rate k_5, and a height of the updraft column equal to 10^4 m.

step of marching calculations by eqs. (1) and (2). Thus we have

$$B = a - k_8 \mathcal{L} \tag{6}$$

where $\mathcal{L} = \overline{m + M}$, with negative values of m taken as zero, and where $k_8 = 0.01 \approx g/\varrho$ is a factor to convert $\mathcal{L}$ to an equivalent acceleration. Although ϱ varies by a factor of about 2.5 through the 10 kilometer depth of calculations described below, the significance of this variation is minimized by our use of average values of water load.

The coefficient k_5, held constant over the model cloud lifetime in the present treatment, was related to element size by Richardson (1926) and called the mixing rate by Priestley (1953). While we recognize that the mixing rate, in nature, certainly varies in both space and time, and is partly self-determined during the evolution of a cloud or storm, we look here for insight from the calculated behavior of updraft columns whose uniform mixing rate is prescribed. The reader may consult more comprehensive discussions by Priestley (1953), by Scorer & Ludlam (1953), and by Turner (1963).

While (5) makes an allowance for the presence of condensate, it also differs from Priestley's similar equation in the presence of the second term on the right-hand side. Its essential effect is to make the value of $w_{\max}$ always drift toward a value close to that attained by an air parcel at $z = H/2$ following its upward (downward) drift from $z = 0$ ($z = H$) in a process represented by $dw/dt = B - k_5 w$. There may be a steady state and when $k_5 = 0$ both eqs. (4b) and (5) assign to $w_{\max}$ the value $w\,(H/2) = (|B|H)^{1/2} \times (\text{sgn } B)$. When k_5 is as large as 10^{-3} sec^{-1}, the steady state values defined by eq. (5) and illustrated in Fig. 1, may be the lower by about 10% in practical cases.

A thermal buoyancy force develops as an air parcel is displaced from its equilibrium level in an atmosphere not neutrally stratified. In the case of continuing rising motion in a column extending upward from the surface, the entire column tends to become composed of parcels originating near the surface, as modified by processes of condensation, precipitation development, and entrainment during ascent. We relate a parameter S_m to the acceleration identified with the average temperature difference between an environmental sounding and the temperature profile associated with ascent of saturated surface air, in the absence of mixing or entrainment. Thus a parcel's thermal acceleration a, is not constant, but a specific average acceleration from thermal causes, S_m, is approached as rising motion of saturated air continues. In parallel with the earlier treatment we look for a simple equation to provide a numerical model that embodies our ideas and suggest

$$\frac{\partial a}{\partial t} = \frac{w_{\max}}{H}(S_m - a) \tag{7}$$

where $H/w_{\max}$ is (somewhat arbitrarily) the time constant. The latent heat of condensation is implicit in (7), and its rate of release is properly proportional to the vertical velocity as shown. Of course there are other factors that affect buoyancy whether there is vertical motion or not. In this model, these are attributed to evaporation of cloud ε_m, evaporation of precipitation ε_M, and a reduction of the thermal component of buoyancy owing to mixing $k_5 a$. Then for the case of rising saturated air we have

$$\frac{\partial a}{\partial t} = \frac{w_{\max}}{H}(S_m - a) - k_6(\varepsilon_m + \varepsilon_M) - k_5 a \tag{8}$$

It remains to extend these considerations to cases of both upward and downward motion of saturated and unsaturated air. The parameters S_m and S_d are introduced accordingly to govern development of buoyancy following vertical motion with and without condensation, respectively. Note now that vertical velocity of either sign is accelerated in unstable cases, decelerated

in stable cases. Thus, in conditionally unstable moist cases or, in absolutely unstable dry cases, the thermal buoyancy approaches positive numbers S_m or S_d respectively, when motion is upward, and negative numbers $-S_m$ and $-S_d$ when motion is downward. Consideration of the various combinations allows us to represent all four cases in the one equation:

$$\frac{\partial a}{\partial t} = \frac{w_{\max}}{H}[F_1 S_m - (1-F_1) S_d - a \operatorname{sgn} w_{\max}] - k_5 a - k_6[\varepsilon_m + \varepsilon_M] \qquad (9)$$

with F_1 the fraction of grid points where cloud exists, each weighted according to its relative contribution to the condensation rate.

It may be noted that in a dry neutral atmosphere without mixing (9) reduces to $(\partial a/\partial t) = -w_{\max} a/H$. Thus an initial buoyancy tends toward zero although mixing is absent. This behavior may seem unrealistic at first thought, but in a neutral atmosphere a local buoyancy should drift toward zero as vertical motion leads to replacement of a buoyant column by neutral environmental air.

S_m and S_d are chosen here so that their sum is 0.4 m/sec².[1] When both are 0.2, for example, the implied tropospheric lapse rate is midway between moist and dry adiabatic values. With a dry adiabatic lapse rate, $S_m = 0.4$ and $S_d = 0$. During marching calculations, S_m is reduced slightly and S_d correspondingly is increased, whenever precipitation evaporation moistens the subcloud layer. This feature accounts for a loss of average buoyancy owing to sensible cooling in the subcloud layer.

The last two terms in brackets account for evaporative cooling. The average rate of evaporation of precipitation, ε_M, is calculated from grid-point values of the term EP in eqs. (1) and (2). Precipitation evaporates only in unsaturated air.

The second term within the last brackets represents the rate of cloud evaporation, calculated where $m > 0$ and averaged over the depth H. This calculation is based on the diminution of cloud as defined by the mixing term in (2). Thus at a particular height we have

$$\frac{\partial m}{\partial t} = -k_5(m - m_0)$$

where $-k_5 m$ represents the dilution of cloud by mixing with saturated cloud free air, and $k_5 m_0$ represents the further depletion that occurs from instant cloud evaporation in unsaturated ambient air (where m_0 is negative). The average cloud evaporation as contrasted to dilution, thus is given by

$$\varepsilon_m = \frac{k_5}{n}[\sum_{m>0} m_0] \qquad (10)$$

where n is the number of grid points in the vertical column and the summation of ambient saturation deficits is derived from all altitudes where the convective column is cloudy.

The coefficient, $k_6 \approx 0.1$ (m/sec²)/(g H_2O/m³), converts the rate of evaporation to the equivalent rate of change of the acceleration attributable to evaporative cooling.[1] The basic equations of our model are (1), (2), (3), (5) and (9).

3. Some elementary properties of the model

In this section we investigate model properties by examining simplified equations. Although these simplifications produce a further departure from reality, they greatly facilitate comprehension of the role of various terms and processes in the complete model, discussed and illustrated in Section 4.

3.1. *Steady state relationships among updraft speed, condensed water load, and buoyancy*

First we should know how the condensed water load, $\mathcal{L}$, tends to vary with the updraft speed, $w_{\max}$, and what values of a tend to exist in the model with associated values of $\mathcal{L}$ and $w_{\max}$. Steady state approximations to eqs. (1) and (2) have been solved by a Runge-Kutta method that can be used whenever $(w + V)$ is everywhere negative. Vertically averaged pre-

[1] The sum represents the buoyant acceleration and associated temperature excess produced by moist adiabatic ascent of surface air without mixing in a dry adiabatic environment. $S_m + S_d = 0.6$ m/sec² is a somewhat better approximation to conditions in a summer thundery atmosphere in the U.S. (surface dewpoint about 20°C). Essential features of this paper are unaffected by variations of $S_m + S_d$ over a considerably larger range.

[2] $k_6 = Lg/C_p T\varrho$, where L is the latent heat of evaporation, C_p is the specific heat at constant pressure, and ϱ is the air density. A comparison of eqs. (5) and (8) with Priestley's velocity and buoyancy equations is given in the parent report.

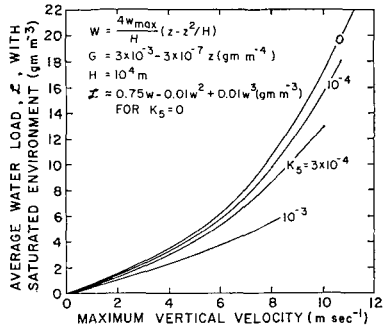

Fig. 2. Average density of cloud + precipitation in a vertical column 10 km high related to maximum vertical air speed and mixing rate k_5. The diagram applies to steady state condition in saturated model updraft columns in saturated environments.

cipitation and cloud content in relation to updraft speeds and values of k_5 are plotted in Fig. 2.

The rapid increase of water load with updraft speed indicated in Fig. 2 implies that in a moist atmosphere, effective buoyancy and updraft probably increase only slowly with increasing thermal component of buoyancy. In Fig. 3, for cases with $k_5 = 0$, we show explicitly how w_{max} depends on the thermal component of buoyancy in a dry model atmosphere, and in a saturated updraft model whose condensed moisture content is illustrated in Fig. 2. It is evident that in the moist case, additional buoyancy is utilized in supporting a relatively large increase in condensation products accompanying a relatively small increase in updraft speed.

It is very important that in a model atmosphere with an elevated condensation level, as shown previously by the author (Kessler, 1969), there are two families of solutions accompanying strong updrafts.[1] In one of these the condensed water load is essentially independent of the updraft speed, and precipitation does not extend to the ground beneath the updraft column. This family is represented by the dashed lines in Fig. 4, applicable to an updraft column 6 km high. In these cases, the model average water load is well defined by the height of the condensation level, with the average temperature or condensation function G, and the mixing rate k_5.

[1] Strictly, this result of kinematic analysis applies to all cases where the formation of precipitation from cloud occurs above and not at the ground surface.

3.2. *Some properties of the buoyancy equation*

The primary control of vertical velocity and hydrometeor development resides in the buoyancy equation (9). Inspection of (9) shows that there is only one source for buoyancy increases in the conditionally unstable model atmosphere, viz., rising motion of cloudy air. Momentum mixing reduces buoyant effects, and evaporation of cloud contributes to negative buoyancy, and both of these processes are independent of the updraft speed in this model. Apparently then, buoyancy can be sustained in cloudy air only if the vertical velocity and associated condensation rate exceed some threshold.

We now explore the associations among k_5, S_m, w_{max}, and m_0, which determine whether the model thermal buoyancy a increases, decreases, or remains steady. Before making numerical calculations based on the complete equations, we use the following simplified form of eq. (8), applicable to rising cloudy air in an environment whose average saturation deficit is $\bar{m}_0$ (a negative quantity);

$$\frac{\partial a}{\partial t} = \frac{w_{max}}{H}(S_m - a) - k_5 a + 0.1 k_5 \bar{m}_0 \qquad (9\,a)$$

We supplement this with

$$a = \frac{w_{max}^2}{H} + k_8 \mathcal{L} \qquad (11)$$

based on a combination of (6) with the steady state form of (5), without the mixing term.

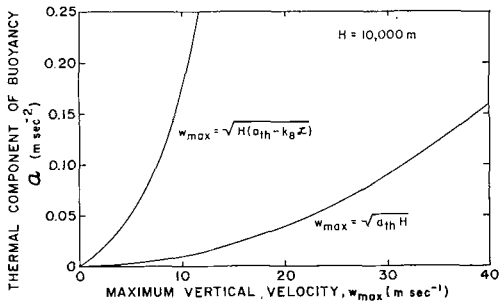

Fig. 3. Thermal component of buoyancy relating to steady maximum velocity in moist and dry atmospheres with no mixing.

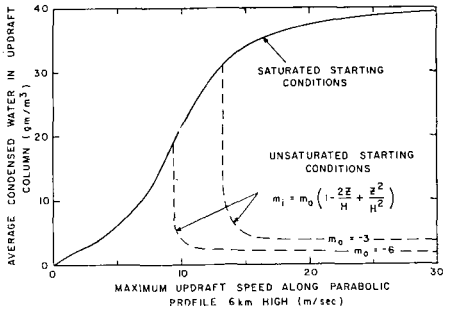

Fig. 4. Vertically averaged steady state condensed water content with maximum updraft speed and initial (ambient) moisture profile, without horizontal mixing (from Kessler, 1969, p. 71).

Relationships between $\mathcal{L}$ and w are of two kinds:

$$\mathcal{L} = 0.75\, w_{\max} - 0.01\, w_{\max}^2 + 0.01\, w_{\max}^3 \qquad (12\,a)$$

$$\mathcal{L} = 5 \qquad (12\,b)$$

The first corresponds to a curve shown in Fig. 2, and the second is a rough approximation for high-speed updraft cases such as illustrated by dashed lines in Fig. 4 (Kessler, 1969).

For parameter values specified by a plotted curve in Figs. 5 and 6, $\partial a/\partial t > 0$ in the region bounded by the curve and the ordinate $\bar{m}_0 = 0$; $\partial a/\partial t = 0$ along a curve, and is negative to its left. This means of course, that the steady condition implicit in our use of eq. (11) is consistent with this analysis only along the curves.

In Fig. 5, where the model environmental lapse rate is everywhere midway between dry and moist adiabatic values (i.e., $S_m = S_d = 0.2$ m sec^{-2}), consider environmental moisture $\bar{m}_0 = -10$. With an average condensed water load of 5 g/m^3, the thermal buoyancy identified with the updraft velocity and water load alone, decreases with time owing to effects of diffusion of buoyancy and evaporation of cloud, unless condensation is produced in an updraft column whose maximum were 7 m/sec or more. If the updraft were a little stronger than 7 m/sec, $\partial a/\partial t$ would be positive, and both a and $w_{\max}$ would increase until the speed of about 34 m/sec were attained. Thus, with other parameters fixed, the magnitude of the initiating disturbance in this conditionally unstable case determines whether the subsequent airflow will decline (as a damped oscillation, see Sec. 3.7) or become the steady updraft condition analogous to Priestley's absolute buoyancy.

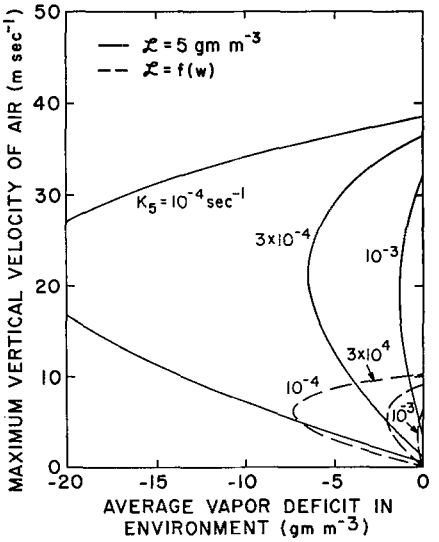

Fig. 5. Loci of $\partial A/\partial t = 0$ in relation to mixing rate, rising air current speeds, and environment moisture, without effects of precipitation evaporation. The family of curves for $L = 5$ simulates high speed updrafts without precipitation beneath; the other simulates updrafts with precipitation at the ground and correspondingly large water loads. The model environment lapse rate is midway between moist- and dry-adiabatic values.

The curves for various values of k_5 may be related to the horizontal dimension of disturbances (see Sec. 5) and they reflect the storage of latent instability in a conditionally unstable atmosphere. They suggest that stronger amplitudes are required with smaller scale disturbances to produce persistent updrafts in conditionally unstable cases. For a specified environmental lapse rate, stronger amplitudes of an initiating disturbance also are required in drier atmospheres. The curves further indicate that for each condition of environmental moisture and lapse rate, there is a size of disturbance below which no perturbation, however large, can produce a persistent updraft.

In Fig. 6, the plots are for various values of the lapse rate, with the mixing rate or size of the disturbance held constant. These lead to inferences, like those discussed above, and moreover reflect the conception that increasing disturbances are necessary to initiate sustained convection as the lapse rate stabilizes.

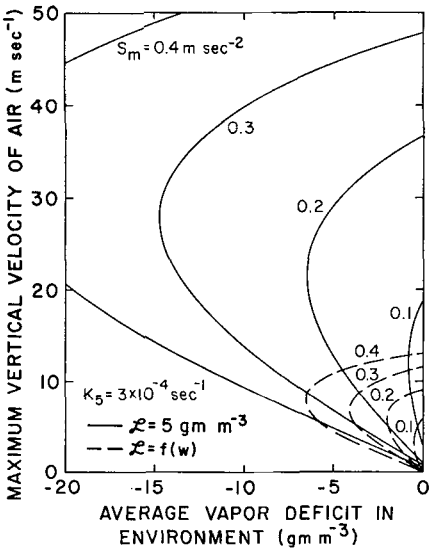

Fig. 6. Loci of $\partial A/\partial t = 0$ relates to environmental lapse rate, the speed of rising currents and environment moisture. The mixing rate is 3×10^{-4} sec^{-1} in all cases. $S_m = 0.4$ m/sec represents a dry adiabatic lapse rate in the environment and $S_m = 0$ represents a moist adiabatic lapse rate.

We should note that an initiating disturbance as a strong determinant of following events is peculiar to conditionally unstable cases. In cases of absolute stability ($\gamma > \gamma_m$) or instability ($\gamma < \gamma_d$), the form of the model solution after a long time depends only on the scale of the phenomenon, and not on the amplitude of an initiating disturbance, as discussed by Priestley.[1]

Of course, forecasters have long thought that strong disturbances, e.g., cold fronts, have an important function in initiating local storms, so this is not a new concept. It is also embodied in others' numerical models. For example, Squires and Turner's model updraft (1962) is sustained only when the upward flux of air at cloud base exceeds a critical threshold.

We should bear in mind that such results are rather critically dependent on the form of the mixing law incorporated into the models. Eventually, we must have models in which the mixing rate is a dependent parameter.

3.3. *Relationships among updraft, water load and rainfall rate during updraft oscillations*

We turn now to fundamental properties of the oscillations involving updraft, condensed water load, and rainfall rate. Byers & Braham (1949) discussed such oscillations in terms of observational data gathered during the Thunderstorm Project, and solutions of various numerical models have since included such oscillations. (For examples see Srivastava, 1971; Weinstein, 1970.) Kessler (1969, pp. 72–73) obtained condensation oscillations as an analytic solution to a pair of differential equations based on inferences from his kinematic study. When such oscillations occur, their approximate period may be

$$T = 2\pi \Big/ \left(k_8 G - \frac{(k_5 - C_3)^2}{4} \right)^{1/2} \qquad (13)$$

where C_3 has the magnitude $|V/H|$ or about 10^{-3} sec^{-1}. It is important that these condensation oscillations do not occur in the model when the water load is independent of the updraft speed. Such independence may occur with a high-speed updraft and an elevated condensation level (see dashed lines in Fig. 4), and the updraft then monotonically approaches a positive value representing equilibrium among forces of thermal buoyancy, water load, and accelerated motions.

In the present numerical context, we first examine the coupled oscillations with $k_5 = 0$, with eqs. (1), (2), and (3) otherwise unchanged, and with eqs. (5) and (9) simplified as shown below:

$$\frac{\partial w_{\max}}{\partial t} = a - k_8 \mathcal{L}; \quad a = \text{constant}.$$

We have used a digital computer with the finite difference forms of the equations to develop solutions of the marching problem. With the simplest case of a saturated model atmosphere, the time variations of $w_{\max}$, surface rainfall rate R_0, and $\mathcal{L}$ for the case where $a = 0.04$ m/sec^2, are shown in Fig. 7. The average period of 1 650 sec, shown in Fig. 7, is very close to that defined by eq. (13).[2]

[1] This statement may be modified for a narrow range of unlikely moist cases in which $\gamma < \gamma_d$ and the mixing rate is large.

[2] With $k_8 = 10^{-2}$ and $G = 1.5 \times 10^{-3}$, eq. (13) yields $T = 1\,636$ sec when $k_5 = 0$ and $C_3 = 10^{-3}$. This agreement is at least partly fortuitous, because C_3 cannot be precisely defined in relation to the more general problem.

Note the excessive rainfall defined by these marching calculations. In light of earlier discussion, it is evident that this combination of a very moist environment with substantial thermal buoyancy is unrealistic. In nature, we expect large vertical heat transports to be triggered before the implied static instability becomes so large.

3.4. *Buoyancy and updraft oscillations*

Fig. 8 shows time variations of vertical air speed for various values of constant thermal buoyancy a, with all other parameters held fixed. In accordance with the analytic theory, the periods and phases practically are unaffected by changes of a. For very large values of a, however, there is a phase shift associated with the nonlinear relationship between updraft speed and water storage. As the updraft speed tends to exceed about 10 m/sec, the locus of maximum water storage is displaced upward to the upper half of the convective column, whence, after the updraft decreases, a longer time is required for descent to the ground. The average updraft speeds and water loads (not shown) with each value of a are close to values along the uppermost curve in Fig. 2.

3.5. *Magnitude of the condensation function and updraft oscillations*

Fig. 9 shows the effect of varying the condensation function in this numerical model. The period of condensation oscillations increases with $1/\sqrt{G}$, as indicated by eq. (13). It would be interesting to test this result by comparing the periods of shower development in warm and cold air masses as revealed by radar echoes.

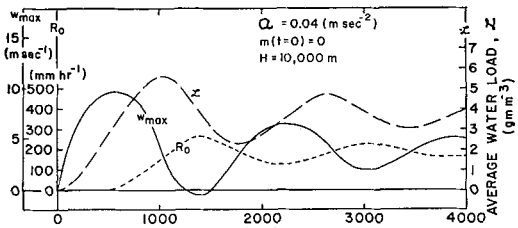

Fig. 7. Mutually dependent oscillations of updraft speed, average water load, and precipitation rate, in a model saturated atmosphere with constant thermal buoyancy and no horizontal mixing.

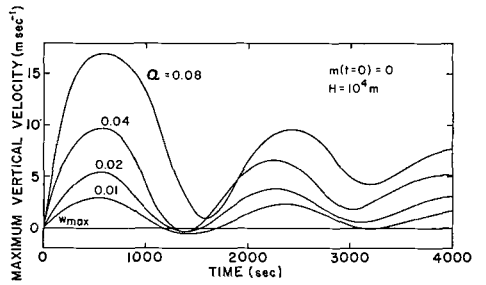

Fig. 8. Updraft oscillations relate to constant thermal buoyancy in a model saturated atmosphere without horizontal mixing.

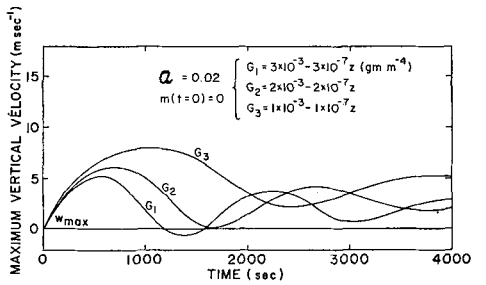

Fig. 9. Updraft oscillations and the condensation function, in a model saturated atmosphere with constant thermal buoyancy and no mixing. The period is very nearly proportional to $1/\sqrt{G}$.

3.6. *Effect of the height of the condensation level in updraft oscillations*

Fig. 10 shows the result of various initial moisture contents when the (constant) thermal buoyancy can produce an updraft speed larger

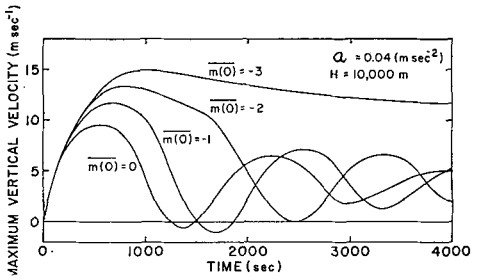

Fig. 10. Updraft development and environmental moisture (average saturation deficit in environment $\overline{m(0)}$), or height of the condensation level, in a model atmosphere with a constant thermal component of buoyancy and no horizontal mixing. Steady updrafts tend to develop as the condensation level rises, provided that thermal buoyancy is sufficiently large.

Table 2. *Period τ of simple undamped oscillations in relation to buoyancy parameter S_d*

S_d (m sec^{-2})	τ (sec)	Approx. equiv. lapse rate[a] (°C/100 m)	Correspondence to dry and moist adiabats: Sfc wet bulb (10°C)	Sfc wet bulb (20°C)
0	∞	1.00	γ_d	γ_d
0.1	1 620	0.95	$.25(3\gamma_d+\gamma_m)$	$.166(5\gamma_d+\gamma_m)$
0.2	1 148	0.90	$.5(\gamma_d+\gamma_m)$	$.333(2\gamma_d+\gamma_m)$
0.3	936	0.85	$.25(\gamma_d+3\gamma_m)$	$.5(\gamma_d+\gamma_m)$
0.4	811	0.80	γ_m	$.333(\gamma_d+2\gamma_m)$
0.5	724	0.75	$.9375\,\gamma_m$	$.166(\gamma_d+5\gamma_m)$
0.6	661	0.70	$.875\,\gamma_m$	γ_m
2.0	363	0	0	0

[a] Based on an assumed mean environmental temperature of about 250 K, and depth $H = 10^4$ m.

than the fall speed of precipitation. As moisture content decreases, the condensation level rises, and the updraft develops longer initially in the longer absence of a substantial water load. (This does not wholly correspond to the more general model discussed in Sec. 4, because delay of condensation adversely affects the development of thermal buoyancy.) The regime of high-speed steady updrafts occurs when an updraft strong enough to hold precipitation aloft develops before significant precipitation forms from cloud. As noted in Sec. 3.3, oscillations are absent in high-speed model updrafts because the water load is practically independent of the updraft speed in these cases (Kessler, 1969 p. 73).

3.7. *Simple oscillations*

The numerical model has simple oscillations (Brunt, 1927) as solutions, as well as condensation oscillations. The simple oscillations correspond to the oscillatory mode discussed by Priestley.

In the case where condensation and mixing are absent and vertical displacements and buoyancy forces are small, eq. (5) becomes

$$\frac{\partial w_{\max}}{\partial t} \approx 1.5\,a \tag{14}$$

which may be equated to d^2z/dt^2 near $z = H/2$, and eq. (9) becomes

$$\frac{\partial a}{\partial t} \approx -\frac{w_{\max} S_d}{H} \tag{15}$$

Integration of (15) and substitution of the resulting expression for a into (14) yields

$$\frac{d^2z}{dt^2} = -1.5\frac{S_d}{H}(z - z_0). \tag{16}$$

In the stable case, $S_d > 0$ and the height of a parcel and all other parameters are then variable with the common period $\tau = 2\pi/\sqrt{(1.5 S_d/H)}$, tabulated in Table 2. Corresponding results of the numerical model discussed in Sec. 4, lie within 10 sec of the tabulated values, suggesting an adequate finite difference scheme.[1]

3.8. *Asymptotic cases and absolute buoyancy*

Priestley denoted the asymptotic case as that where, although the lapse rate is unstable, an initiating perturbation is monotonically reduced to zero. This trend responds to effects of mixing, analogous to the effects of molecular viscosity and conduction treated in classical papers. Our equations admit similar solutions.

Consider eqs. (5) and (9) in relation to updrafts in a dry atmosphere, i.e., $w \geq 0$ and $\mathcal{L}$, F_1, ε_M and ε_m all identically zero. Then we have

$$\frac{\partial w_{\max}}{\partial t} = 1.5\left[a - \left|\frac{a}{H}\right|^{1/2} w_{\max}\right] - k_5\, w_{\max} \qquad \text{(5, dry form)}$$

[1] When mixing is present, the period is $\tau = 2\pi/[(1.5 S_d/H) - k_5^2/4]^{\frac{1}{2}}$ and so essentially is unaffected by values of k_5 much smaller than those associated with critical damping.

$$\frac{\partial a}{\partial t} = \frac{w_{\max}}{H}(S_d + a) - k_5 a \tag{9 b}$$

With $\partial w_{\max}/\partial t = \partial a/\partial t = 0$, steady state relationships are defined, viz.,

$$S_d = -k_5[(aH)^{1/2} + \tfrac{2}{3}k_5 H] - a \tag{17}$$

and

$$w_{\max} = -\frac{k_5 H a}{S_d + a} \tag{18}$$

The limiting value of S_d for steady upward motion is given by eq. (17) with $a = 0$. Thus, steady states analogous to Priestley's "absolute buoyancy" occur when $S_d < -\frac{2}{3}k_5^2 H$ i.e., for sufficiently unstable lapse rates. Only when the magnitude of S_d is larger than the indicated threshold can any disturbance, however small, be associated with the monotonic increase of vertical velocity toward an asymptote of vertical velocity defined by (18). Eq. (17) is not satisfied by smaller magnitudes of absolute instability denoted by negative values of S_d; smaller negative magnitudes are associated with reduction of disturbances to zero.

Inspection of eqs. (5) and (9) shows that asymptotic cases should also occur in a saturated atmosphere whose lapse rate exceeds the moist adiabatic; since the water load is closely related to updraft speed when updrafts are weak, condensation oscillations alter the solutions from the monotonic behavior of the dry case. Also, since the water load opposes buoyancy, we expect the asymptotic boundary to lie further from $S_m = 0$ in moist cases than from $S_d = 0$ in dry cases. Because of the great complexity of the moist equations, we have not attempted a detailed analytic study of the moist asymptotic family, but a numerical solution is illustrated in Sec. 4 (Fig. 13).

4. Solutions of the complete numerical model

4.1. *General comments*

Finite difference calculations based on the complete model have been made with many values of the regulating parameters and a 41 gridpoint column. The computer program uses forward time differences and centered space differences and simply expands the version described by Newburg & Kessler (Kessler, 1969, p. 80).

The following discussion deals exclusively with cases where the updraft is initiated by a starting perturbation buoyancy, i.e., an initial assigned value of a. Subsequent development in conditionally unstable situations may depend largely on the magnitude of this input parameter for reasons discussed in Sec. 3.2.

We describe five types of solutions given by the model, viz. (*a*) in stable dry cases, simple damped oscillations; (*b*) in moist stable or conditionally unstable cases, cloud and precipitation development leading to a shower (a kind of condensation oscillation), followed by damped simple oscillations; (*c*) an updraft that becomes steady, and is accompanied by steady rain at the ground; (*d*) an updraft that becomes steady and strong (15–40 m/sec) without precipitation beneath, but, in a moist atmosphere, with precipitation implied outside the area beneath the strongest updraft; and (*e*) with weak absolute instability, disturbances restored monotonically and asymptotically to zero when the mixing rate is sufficiently large. With larger absolute instability than type (*e*), steady updrafts with cloud and precipitation (types (*c*) and (*d*)) develop in a moist model or sustained updrafts without cloud in a dry model.

The types of solution tend to drift from simple damped oscillations toward high speed updrafts as the environmental lapse rate and the perturbation buoyancy increase, and as the mixing rate decreases, i.e., as the implied horizontal dimension of the updraft area increases. With a given conditionally unstable lapse rate, the shower mode is less favored and a steady mode more favored when the moisture content of the environment is high, but steady high speed updrafts are most favored by less-than-saturated moisture conditions, i.e., by a somewhat elevated condensation level, or by a large threshold for cloud conversion (large value of a in the autoconversion term AC in eqs. (1) and (2)). The transitions between some solution types appear to be discontinuous for changes of input parameters across thresholds, as suggested by the discussion in Sec. 3.2. Simple damped oscillations and showers correspond to Priestley's oscillatory solution and the steady updraft cases to his "absolute buoyancy".

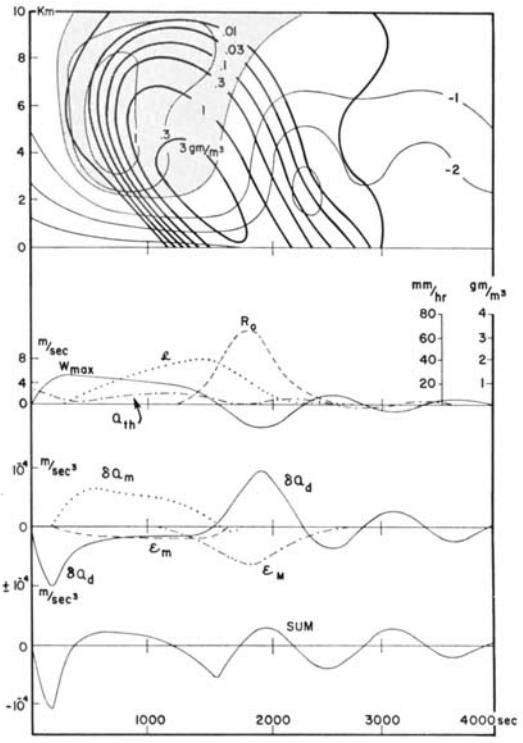

Fig. 11. Development of cloud, precipitation, buoyancy, and updraft speed in a weakly perturbed model atmosphere.

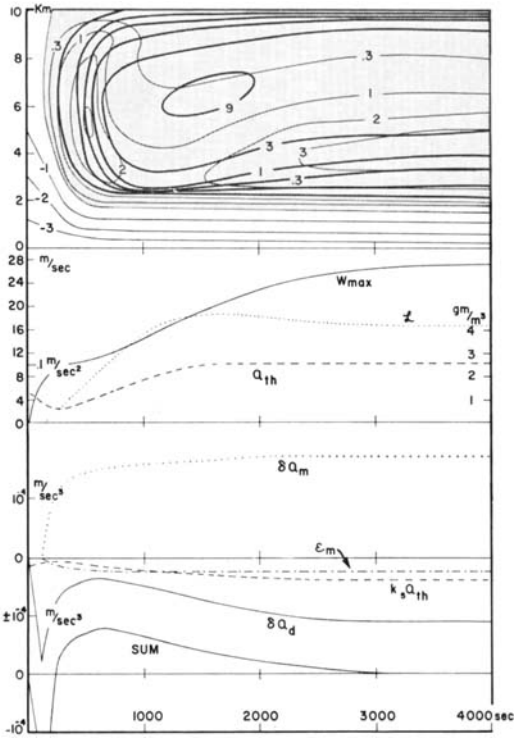

Fig. 12. Development of hydrometeors, buoyancy and updraft speed in a model atmosphere with a starting thermal perturbation twice as large as illustrated in Fig. 11.

4.2. *Sample solutions*

Several solution types are represented in Figs. 11 and 12. Among the parameters used in the calculations, only the starting perturbation buoyancy is different in these two cases. Other parameters are as listed in Table 1 and as follows: mixing rate $k_5 = 3 \times 10^{-4}$ sec^{-1} corresponding to a cell diameter of about 8 km (see Fig. 17); environmental and starting moisture $m_0 = 4 + 8 \times 10^{-4}z - 4 \times 10^{-8}z^2$ (g/m^3). The perturbation buoyancies corresponding to Figs. 11 and 12 are 0.025 m/sec^2 and 0.05 m/sec^2, respectively, and are equivalent to average starting temperature excesses of approximately 0.7 and 1.4°C.

At the top of Fig. 11 is a time-height portrayal of the development of cloud, precipitation, and vapor distributions in the weak perturbation case. Beneath that, on the same time scale, the magnitudes of the maximum updraft, average condensed water load, and rainfall rate at the ground are plotted with the thermal component of buoyancy. The third series of plots illustrates terms contributing to $\partial a/\partial t$. The plot of δa_m represents $(w_{\max}/H)[F_1 S_m - a \times \operatorname{sgn} w]$ in eq. (5), or the effect of vertically moving cloudy air. The plot of δa_d represents $-(w_{\max}/H[(1-F_1)(S_d) + a \times \operatorname{sgn} w]$ or the effect of vertically moving unsaturated air. The contributions of vertically averaged evaporation of precipitation and cloud are represented by ε_M and ε_m. The fourth plot represents $\partial a/\partial t$ or the sum of all contributions to change of thermal buoyancy, including small values of $-k_5 a$ not separately depicted.

In physical terms, the development of updrafts and hydrometeors in the complete model, Fig. 11, is regulated as follows: an upward air current develops immediately after the start in response to the input perturbation thermal buoyancy. The thermal buoyancy immediately starts to decline, partly as a result of mixing

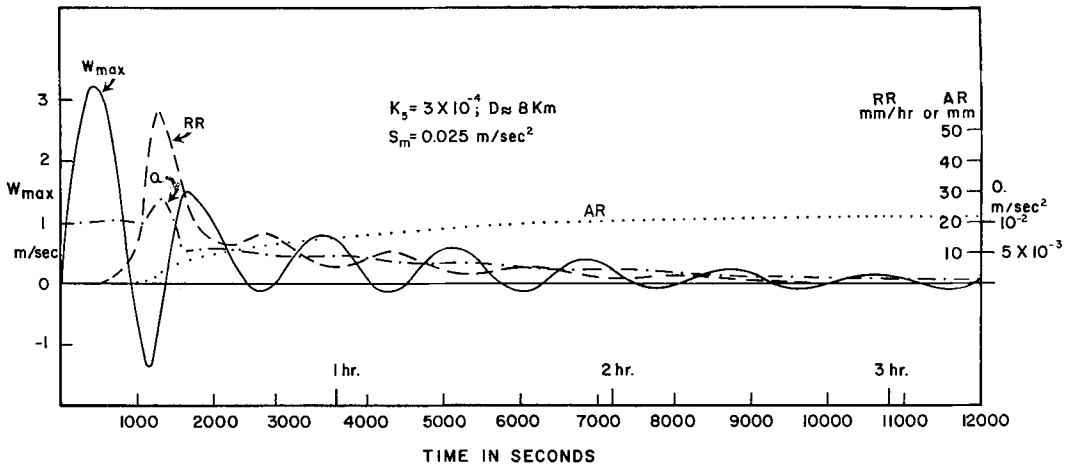

Fig. 13. Updrafts, thermal component of buoyancy, precipitation rate at the ground, and accumulated precipitation in relation to time in a saturated model atmosphere with a super-moist adiabatic lapse rate. The decline of updrafts to zero, analogous to Priestley's asymptotic cases, is accompanied by condensation oscillations in the moist model.

of updraft air with environmental air ($-k_s a$), but more because the environmental lapse rate is stable for vertical motions of dry air (δa_d). As saturation is attained, condensation occurs. Then the term δa_d decreases and δa_m becomes a prominent contributor to positive buoyancy in the examples given, since an appreciable vertical velocity accompanies condensation. The thermal buoyancy then declines less rapidly and, indeed, the thermal component increases again after 300 sec. The increase corresponds to a rapid addition of heat from condensation, exceeding the rate of loss of sensible heat by mixing ambient and environmental air and evaporating cloud.

Meanwhile, however, condensation products are accumulating in the updraft column, and since the effective buoyancy is related to both its thermal component and water load, this increase of condensation products additionally effects the updraft. In Fig. 11, the rate of increase of condensation products more than offsets the rate of increase of thermal buoyancy, and after 300 sec produces decreasing effective buoyancy ($a - k_s \mathcal{L}$), and diminishing updraft speed. By now substantial amounts of precipitation have formed in the updraft column, and as the updraft weakens, descent of precipitation toward the ground is hastened. When precipitation falls into the subcloud layer, there its partial evaporation produces a substantial contribution to negative thermal buoyancy. (See also Syono & Takeda, 1962 and Das, 1964.) The downdraft (Fig. 11) starting at about 1 600 sec is attributable to dominant water load effects, in the presence of a residual small positive thermal buoyancy.

As precipitation falls rapidly out of the descending air column and the cloud evaporates, we have the case of descending dry motion in a stable environment, and a restoring upward buoyancy increases. The subsequent record is that of a simple oscillation.

We note in passing that in such cases, one effect of hastened transformation of cloud to precipitation is a reduction of the total amount of precipitation deposited on the ground. The reduction occurs because the updraft, the ultimate source of precipitation in the model, suffers an earlier reduction of buoyancy owing to precipitation evaporating in the subcloud layer.

The early developments illustrated in Fig. 12 are similar to Fig. 11. Because of the stronger starting thermal perturbation, however, the vertical velocity is larger in Fig. 12 when condensation begins. This produces a more rapid recovery of thermal buoyancy, whose rate of increase exceeds the contrary tendency of the increasing water load. Therefore, the updraft continues to increase, precipitation is held aloft, and the high-speed steady updraft case develops. The precipitation aloft diverges there, and

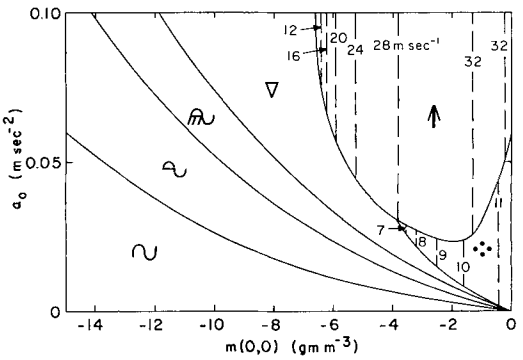

Fig. 14. Types of solutions of the complete numerical model in relation to environmental moisture and starting thermal perturbation. Simple oscillations (Type *a*) appear at lower left, solitary showers (Type *b*) are indicated by a triangle, high-speed updrafts without precipitation beneath (Type *d*) are indicated by an arrow, and continuous precipitation at the ground (Type *c*) is represented at the lower right. Isopleths in the right side of the figure indicate the steady values of maximum vertical velocity ultimately attained with solution Types *c* and *d*. All illustrated solutions apply to a lapse rate midway between moist and dry adiabatic values for mixing rate $k_5 = 3 \times 10^{-4}$ sec^{-1}.

descent toward the ground is implied in adjacent regions where the updraft is not so strong.

Fig. 13 illustrates the numerical solution of a moist absolutely unstable case. Here the environment is completely saturated and $S_m = +0.025$ m/sec^2, corresponding to a maximum attainable average excess temperature in the ascending column of about 0.6 C. With a starting perturbation $a_0 = 0.01$ m sec^{-2} and a mixing rate of 3×10^{-4} sec^{-1}, updrafts attain a maximum value near 3.5 m/sec, and a rainfall rate of 55 mm/h occurs; then in about 3 hours these and associated parameters decrease to negligible values. Total rainfall beneath the model updraft column in this example is about 22 mm. When the model instability S_m is sufficiently increased, or the mixing rate k_5 is reduced while a saturated environment is maintained, updrafts and other parameters drift through the regime of damped condensation oscillations toward a condition of steady updrafts with heavy rain beneath. A development of rain at the ground rather than a high speed updraft case may depend also on microphysical processes so active, or updraft development so slow that precipitation forms before the updraft speed has attained the speed at which precipitation falls. With faster updraft development or slower cloud-conversion processes, the end result tends toward high speed updrafts without precipitation beneath, when instability is great.

Because we have not accounted for a stabilization of the atmosphere necessarily associated with the rapid ascent of part of it, the examples given may be thought to exaggerate the intensity and duration of events. Thus, the perturbation buoyancy used for Fig. 11 may lead to little or no rain in a more comprehensive model, and Fig. 12 would more logically portray vertical motion of limited duration. Nevertheless, implications of this study of perturbation buoyancy effects may still be valid. The weaker perturbations would tend to be damped, and the duration of events established by the stronger perturbations should depend on the strength of sources of fresh air similar to that overturned in the convective process.

4.3. *Distribution of solution types in relation to model input parameters*

The distribution of solution types shown in Fig. 14 corresponds fairly to our expectations based on Sec. 3.2. Along the abscissa is the initial and environmental moisture content at $z = 0$, i.e., the magnitude of C_0 in the equation $m = C_0 - (2C_0/H)z + (C_0/H^2)z^2$. The starting perturbation is plotted along the ordinate. Interior lines show the loci of the solution types referred to in Sec. 4.1, when all parameters except those indicated on the ordinate and abscissa are as given in Sec. 4.2.

As the mixing rate k_5 declines, the area occupied by high speed updrafts in a diagram like Fig. 14 increases, as suggested by Fig. 5. Increasing the autoconversion threshold has a similar effect, since this both reduces the accumulation of condensation products and increases the effective buoyancy.

An alternate presentation, Fig. 15, represents the development of vertical velocity with conditions depicted by an ordinate value $a_0 = 0.025$ in Fig. 14. The upper shaded area in Fig. 15 presents the condition of continuing precipitation at the ground, and the lower shaded area falls in Fig. 14's region of showers. Between these two lie cases of high-speed updrafts without precipitation at the ground beneath the strongest updraft. Below the shower area in

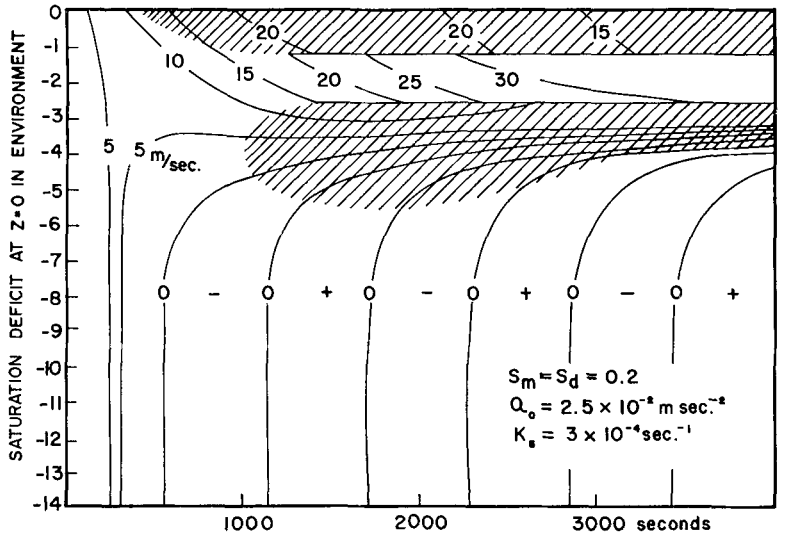

Fig. 15. Vertical velocity and precipitation at the ground (shaded areas) in relation to time, with a starting perturbation $A_0 = 0.025$, and environmental moisture content. Ordinate values represent C_0 in the equation $m_0 = C_0 - 2 \times 10^{-4} C_0 z + 10^{-8} C_0 z^2$.

the diagram, the air motion is fairly described by the theory of simple oscillations.

Since these results are quite dependent on the mixing law somewhat arbitrarily chosen, the further theoretical development of mixing models applicable to large cumulus clouds plus the testing and refinement of this aspect of the model should have high priority.

As one possible analysis involving the microphysical parameters, we illustrate how change of the particle-size distribution affects the distribution of solution types. If N_0 were 10^5 m^{-4} instead of 10^7 m^{-4} as in Fig. 14, the particle sizes for the same water content would be increased by a factor $100^{0.25} = 3.162$. Other factors would also change, however. The faster fall speeds of the larger particles ($V \propto N_0^{0.125}$) would be associated with a greater fallout and diminished precipitation content M. On the other hand, the accretion rate of precipitation for cloud would be smaller ($AC \propto N_0^{0.125}$), because of the less numerous particles; cloud density m would rise and the net decline of $\mathcal{L}$ would be less than that of M. For cases where precipitation falls into the subcloud layer with the smaller value of N_0, the rate of evaporation of precipitation in that layer would be reduced since $EP \propto N_0^{0.35}$, but it is obvious that EP effects on the buoyancy would be larger if some evaporation occurred where previously there had been none. The complicated interactions of these and some other model processes are automatically accounted for when calculations are made with the changed value of N_0. Results of about 30 such marching calculations have been the basis for Fig. 16, which shows a larger area of steady precipitation and a smaller area of high-speed updrafts than in Fig. 14. Implications in Figs. 14 and 16 have possible significance for those who strive to reduce the incidence of damaging hail. Further model developments should help to clarify whether hail formation affects updraft intensity and surface winds in real storms.

5. Comments on thunderstorm size and boundary layer effects on storm development

5.1. *Size in relation to mixing rate*

The parameter k_5 can be related to the size of the updraft column. This appears worthwhile, although the accuracy of our indication may be little better than an order of magnitude. The equation proposed by Richardson (1926) and subsequently used by Priestley becomes in mgs units

$$k_5 = 0.117 D^{-2/3} \text{ sec}^{-1} \qquad (19a)$$

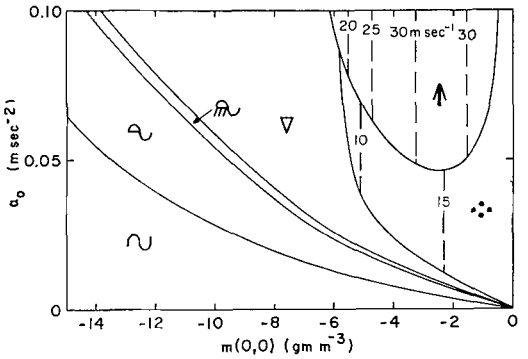

Fig. 16. Same as Fig. 14, except the drop-size distribution parameter N_0 is 10^5, and the precipitation formed aloft corresponds in size, fall speed, and some other characteristics to small hail.

or

$$D = 0.04k_5^{-3/2} \text{ m} \tag{19b}$$

where D is the diameter of a cylindrical column. This relationship is plotted in Fig. 17.

5.2. *A critical Richardson Number in relation to storm size and intensity*

In Secs. 3.2 and 4, we discuss concepts of a critical size and buoyancy required to initiate sustained updrafts. We need further to inquire into criteria for a maximum size and in this connection it seems that an effect of a circulation on itself may be significant. A vertical current associates with inflow below and outflow above, hence with a vertical shear of the horizontal winds; Richardson (1920) gave us a criterion for the breakdown of a vertically shearing current.

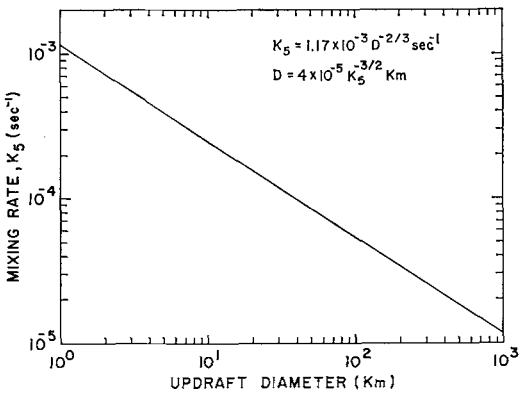

Fig. 17. Horizontal extent of a rising column vs. mixing rate, according to an equation used by Priestley (1953).

Consider a cylindrical column of radius R and height H. At the height $H/2$, we assume that the updraft is $w_{\max}$. The flux through the level $H/2$ is thus $\pi R^2 \varrho_m w_{\max}$ and continuity requires that this be matched by an inward flux of air below the level $H/2$. Then

$$\pi R^2 \varrho_m w_{\max} = 2\pi R \frac{H}{2} \varrho_b \bar{u}_i$$

and

$$\bar{u}_i = \frac{R w_{\max}}{H}$$

if we neglect the difference between ϱ_m and ϱ_b, the air densities at the middle and in the lower half of the column. Above the level $H/2$, an equal outward flux is associated with the wind speed $\bar{u}_0$. Then the average shear of the horizontal wind is

$$\frac{\Delta u}{\Delta z} = \frac{\bar{u}_0 - \bar{u}_i}{H/2} = \frac{2Dw_{\max}}{H^2} \tag{20}$$

and a Richardson Number involving mean quantities is

$$R_i = \frac{\dfrac{g}{\bar{\theta}} \dfrac{\Delta\theta}{\Delta z}}{(\Delta u/\Delta z)^2} = \frac{gH^3\Delta\theta}{4\bar{\theta}D^2 w_{\max}^2} \tag{21}$$

where $\Delta\theta$ is the difference of potential temperatures between height $z = h$ and $z = 0$, and D is updraft column diameter. Inclusion of density variations in the analysis introduces the term $\varrho_m(\varrho_a + \varrho_b)/\varrho_a\varrho_b$ to the numerator of the right side of (20). The shear is then increased by about 5% when H is as large as 10^4 m, and the Richardson Number is correspondingly reduced by 10%.

Richardson proposed the value $R_i = 1$ as the criterion for an increase of a turbulent perturbation although we recognize now that parameters other than R_i are important with respect to turbulent growth and spread (Pao & Goldburg, 1969). Atmospheric turbulence usually seems to be initiated with $R_i \approx 0.25$, but we may use the value unity because real circulations are associated with substantial irregularities.

Although this discussion is extended in the parent report, the author only suggests here a plausible mechanism for defining gross characteristics of convective cell size and intensity. As cells grow, they should become more susceptible to breakdown by turbulence of their own making. A rough analysis including consideration of the role of condensed water on effective buoyancy indicates that a trend from weak large cells to strong small cells should be associated with a trend toward a less stable ambient stratification. We proceed uncertainly, however, since it is not clear in conditionally unstable cases whether the potential temperature or wet bulb potential temperature should be applied in (20). It seems that large intense storms should occur when the mid-troposphere is dry with a lapse rate nearly midway between moist and dry adiabats, and when the boundary layer provides great masses of moisture. Then the ambient lapse rate is steep enough to drive the condensing convective column at great speed as well as stable enough to resist breakdown by the shears thus created. With a dry environment, a large size is required for convection to be maintained against dissipating mixing effects. Fig. 18 illustrates that convective cells' characteristic size and intensity varies with the air mass.

5.3. *Some inferences for storm behavior and empirical tests*

We give here a rather speculative topical commentary on thunderstorm behavior as it is or may be, in light of our model.

(1) *Role of initiating disturbances.* These are emphasized in this theory. Unless the horizontal dimension and amplitude of an initiating disturbance are above specific values that depend on environmental parameters, sustained model convection does not occur. We are, therefore, in forecasting led to renew our surveillance of possible disturbance sources and to examine data that can shed more light on the connection between starting disturbances and real showers and thunderstorms.

(2) *Diurnal and geographic variations of storm behavior.* The maximum frequency of thunderstorms and tornadoes over most of the United States occurs during the evening hours rather than during the hottest part of the day at the ground (Flora, 1954; Rasmussen, 1970); Rasmussen has discussed some theories already proposed to explain this behavior, and part of his comprehensive analysis of data is illustrated here in Fig. 19. Consider that during the early afternoon, the horizontal dimensions of disturbances in the planetary boundary layer (PBL) are apt to be small because of a steep lapse rate in that layer. Then we expect towering clouds that develop to be small proportionate to their roots, and to suffer correspondingly large losses of buoyant energy by entrainment of ambient air. During evening and at night, however, the boundary layer becomes internally stable, while often it retains its essential warmth with respect to higher layers. Then larger convergence areas may exist in the PBL without breakdown, and the PBL should also then admit gravity waves whose propagation and superposition may be significant for initiating sustained deep convection. A related effect in the PBL may contribute to the observed diurnal variation of convective storms: the stronger coupling of a deep air layer with terrain at midday should hinder involvement in deep convection of the boundary layer air, the principal reservoir of vigorous storms' energy and moisture.[1]

Fig. 19 shows that early afternoon storms are prominent along the Gulf Coast, in the Rocky Mountains, and in the Appalachian Mountains. Mountain topography provides discrete heat sources at the ground that should promote overturning during the hottest part of the day on the scale of topographical irregularities. With regard to the afternoon maximum of thunderstorm activity along the Gulf Coast, indicated in Rasmussen's data, we note that our theory indicates that smaller scale convection can be sustained in moister atmospheres. Thus, the smaller scale convection inferred for the unstable boundary layer, characteristic of midday, may give rise to absolute buoyancy when the air is sufficiently moist. Furthermore, along the Gulf Coast the early maxima should be promoted by the sea breeze, and in Florida by peninsula-induced convergence (Frank et al., 1967).

(3) *The highly turbulent nature of thunderstorms.* Our application of Richardson's theory suggests a fresh view of storm turbulence. The

[1] We propose too that the rapid changes of cloud forms commonly witnessed in late afternoon over land areas are associated with a rapid transition from an unstable boundary layer strongly coupled to terrain, to a thin stable layer overlain by a warm, moist, deep decoupled layer.

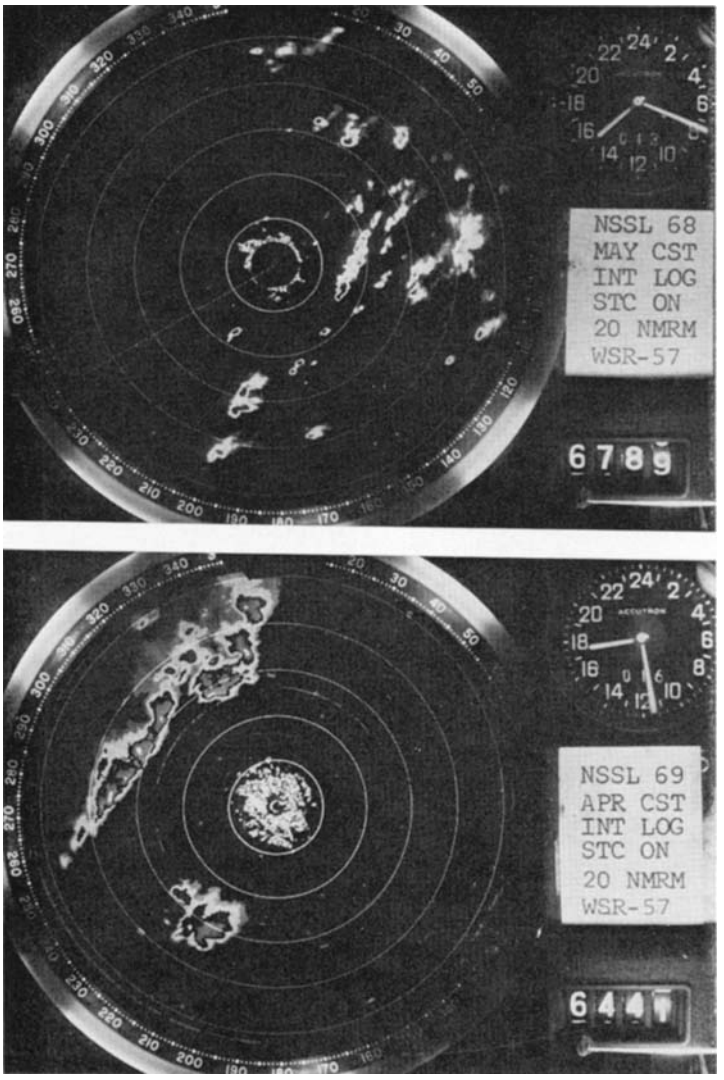

Fig. 18. Photographs of the PPI display of the NSSL WSR-57 radar, May 13, 1968 (top) and April 16, 1969. Range marks are at intervals of 20 n mi. The size of cells within a group may associate with a moist conditioning of air, by the cells themselves, requiring an approximation to $\Delta\theta_w$ in eq. (2) in place of $\Delta\theta$. Cell sizes and intensities appear characteristic of the occasion, and presumably, the air mass.

air in the environment of a storm may be nonturbulent in the presence of its own vertical shear because it is only conditionally unstable. When this air is sufficiently lifted by storm circulation, however, it becomes cloudy and its Richardson Number becomes zero or negative. Then its vertical shear would contribute to the amplification of ubiquitous small disturbances. The shear of the environment would act also to induce some shear in the warm air column rising from low altitudes in the storm core, with promotion of the multi-turreted boiling appearance so characteristic of storms.

We might use aircraft and Doppler radar to investigate the turbulence within storms related to the vertical shear in the storm environment.

(4) *Right- and left-moving storms, and storms that split.* Severe storms commonly move markedly to right or left of the mean-layer winds; right-movers are more frequent. Explanations

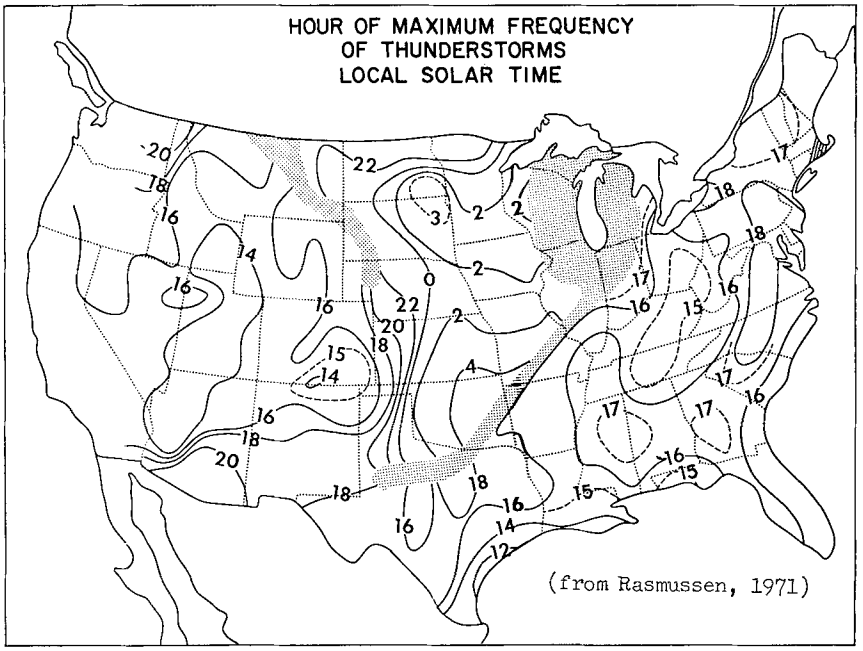

Fig. 19. Local solar time of maximum thunderstorm frequency over the United States (Rasmussen, 1971)

have involved availability of atmospheric moisture and dynamic effects of storm rotation (Newton, 1960; Fujita, 1969; Charba & Sasaki, 1968; Kuo, 1970). We note particularly Fankhauser's (1971) discussion of one of the class of storms that move while not severe with the wind, and to the right of the wind while severe. During a nonsevere period, we expect the horizontal momentum of storm air to adjust more nearly to the average in the environment because its slower ascent gives it more time to do so. During a severe period, however, the more rapid replacement of storm air by fresh low-level air would associate with a greater difference between the horizontal motion of storm air and environmental air, with more of a barrier effect. Then the air at mid-levels would tend more to flow around the storm with its speed enhanced by the Bernoulli effect (Fig. 20). Then the largest vertical shear would be in areas on the storms' southeast and northwest sides; and always-present local disturbances would, by Richardson's criterion, be most prone to grow in these areas. Investigators have noted that right- and left-moving storms actually are associated with new cell development on their southeast and northwest sides, respectively (Browning, 1964; Haglund, 1967; Hammond, 1969). Of course, we must discover what favors development on either one or the other of southeast or northwest sides of existing cells.

Radar observations of storms often show a splitting into right- and left-moving parts (see Fankhauser, 1971, fig. 20). The storms that split and their fragments are often large and intense. Perhaps the splitting occurs in part as an effect of the circulation on itself, as suggested in Sec. 5.2.

(5) *The size of storms.* Our model admits sustained small-element convection in a very moist atmosphere whose lapse rate exceeds the moist adiabatic, and in a dry atmosphere with a superadiabatic lapse rate. With intermediate values of lapse rate and moisture, sustained convection occurs only when elements are large, so that the mixing rate and cloud evaporation losses into the dry ambient air are small. Very strong updrafts may develop in a conditionally unstable case when moist elements are large, because the rising column is then much warmer than its surroundings and the statically stable dry environment resists breakdown. Thus, does the theory explain predominance of large intense storms where a lower moist layer is capped by a deep dry layer?

(6) *Propagation of storms.* Sometimes severe

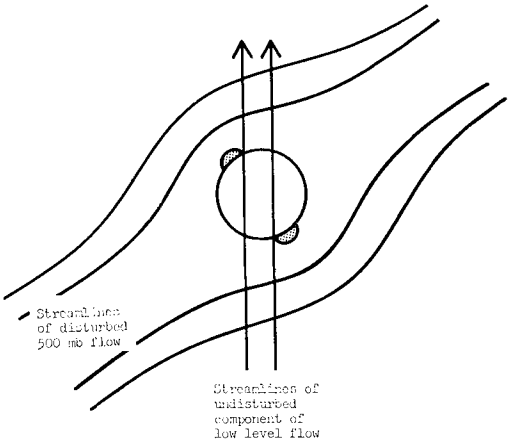

Fig. 20. If a severe storm acts as a barrier in potential flow, a typical southwesterly flow aloft would be most increased in the shaded areas northwest and southeast of the storm. The intensified vertical shear might provide energy for amplification of vertical disturbances in these areas, identified with new development in left- and right-moving storms, respectively (Hammond, 1967; Haglund, 1969; Fankhauser, 1971, esp. his figures 6B and 16).

storms and showers move ahead of the cold front often identified as their primary cause, while on other occasions, the storms may remain along the causal front. In terms of our theory, the latter condition, storms along the front, would be identified with cold front disturbances which, in some sense, have subcritical size and/or amplitude.

In a conditionally unstable air mass that is practically uniform horizontally, the largest disturbances ahead of a storm line may be produced by already-existing storms. In addition to the well-known effect of cold air underrunning, we consider the storm circulation effect to change the vertical wind shear near the storms. Then the propagation of storms, i.e., the direction of development of new storms, may be toward the place where the vertical shear is enhanced locally, and the pace of storm propagation should depend on the environment's instability and already existing shear. It seems worthwhile to investigate the Richardson Number as a forecasting parameter.

6. Concluding remarks

The principal results of this work are outlined in the Abstract and discussed in Secs. 4 and 5. Our forms of model convection are summarized in Fig. 21.

This model emphasizes the importance of substantial disturbances as initiators of sustained convection in conditionally unstable cases. Thus, we sense confirmation of the widely held belief that more accurate forecasting of convection largely will depend on more detailed observations of percursor phenomena. Improved theories should indicate types of weather data needed for application to storm-forecasting operations.

It may be worthwhile to explore further some features of the model. For example, solutions might be obtained with various shapes of environmental moisture profiles. The model might evaluate further the atmosphere's storage of its instability against the occurrence of a disturbance of sufficient amplitude and horizontal size. Atmospheric data might be studied to evaluate environmental shear in relation to the propagation of real storms: the development of storms in real cases should be investigated in light of combined effects of large-scale disturbances and boundary layers.

Other examples include more realistic treatment of hail by increase of the drop-size parameter N_0 during descent of precipitation through a melting level. And with carefully designed constraints, the parabolic vertical velocity profile might be replaced by a distribution more indicative of local, rather than average, buoyancy. But the first modification would probably not change the conclusions substantially nor significantly enlarge their scope. The second would probably affect the answers considerably, but a model so simplified with respect to entrainment processes and other environmental effects should not be carried very far.

Perhaps more important now than *ad hoc* model improvements are further theoretical and experimental examinations of entrainment mechanisms, of the turbulent breakdown or growth of organized disturbances, of energy dissipation in the boundary layer, and of the coupling between the boundary layer and higher layers. These processes and relationships must be critical ingredients of a realistic numerical model of time-dependent deep moist convection in a two- or three-dimensional space.

Finally, we emphasize that a great virtue of a numerical model is its susceptibility to improvement based on empirical tests and theore-

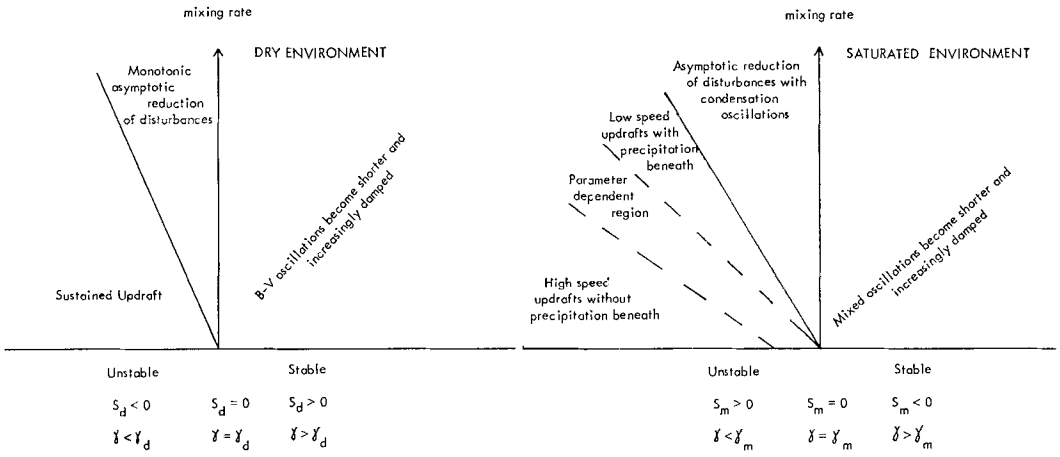

Fig. 21. Modes of model air motion, lapse rate and mixing rate in dry and saturated model environments. Boundaries of the parameter-dependent region depend on the amplitude of model disturbances and microphysical processes. Complicated conditionally unstable cases are discussed in Section 4.3.

tical reasoning. Contemporaneous study of storm models and observational data can provide guidance and more rapid evolution of new knowledge.

Acknowledgements

Mr William Bumgarner produced remarkably efficient computer programs and greatly aided the model design. Dr Rex Inman, Oklahoma University, noted the relationship of two of the basic equations in this paper with Priestley's earlier model, at an intermediate stage of the investigation. Dr Edward A. Newburg, Virginia Commonwealth University, provided guidance to the solution of differential equations by finite differences. Various useful suggestions also were provided by Professor Frank H. Ludlam of Imperial College, London; and Professor Fred Sanders of MIT, Cambridge, Massachusetts; and Mr Pieter Feteris and several others at the National Severe Storms Laboratory. Mrs Helen J. Ardrey of NSSL was a helpful editor; Ms Brenda Courtney took good care of the typescript.

Appendix

The following derivations of the buoyancy eq. (5) and of the tendency eq. (9) have been given by Dr Robert Davies-Jones of NSSL.

In one-dimensional cloud models, the vertical equation of motion is

$$\frac{\partial w}{\partial t} + w\frac{\partial w}{\partial z} = B - k_5 w \tag{i}$$

where $B = g[(T_v - T_{ve}/T_v) - k_8(M+m)]$ and Priestley's mixing is assumed. For updrafts we integrate (i) between $z=0$ and $z=H/2$ and obtain

$$\frac{\partial \overline{w}}{\partial t} + \frac{w^2\left(\frac{H}{2}\right)}{H} = \overline{B} - k_5\overline{w} \tag{ii}$$

where $\overline{(\quad)} = (2/H)\int_0^{H/2}(\quad)\,dZ$. We further assume the parabolic profile (4) whence $w(H/2) = w_{\max}$ and $\overline{w} = 2/3\, w_{\max}$. Then

$$\frac{\partial w_{\max}}{\partial t} = 1.5\left(\overline{B} - \frac{w_{\max}^2}{H}\right) - k_5 w_{\max} \tag{iii}$$

Equation (iii) is derived rigorously but is nonlinear. To linearize, we assume a quasi-steady state with small mixing so that

$$w_{\max} = \sqrt{H\overline{B}} + w'$$

where $w' \ll \sqrt{H\overline{B}}$. Let $e \equiv w'/\sqrt{H\overline{B}}$. Then to first order accuracy in e,

$$\frac{w_{\max}^2}{H} \sim \sqrt{\frac{\overline{B}}{H}}\, w_{\max},$$

and (iii) becomes

$$\frac{\partial w_{\max}}{\partial t} \approx 1.5\left(\overline{B} - \sqrt{\frac{\overline{\overline{B}}}{H}}\, w_{\max}\right) - k_5 w_{\max} \qquad (5)$$

For a downdraft, integration is between $z = H/2$ and H with appropriate sign changes.

A starting point for derivation of eq. (9) in our text is given by Priestley's tendency equation for the buoyancy:

$$\frac{\partial T'}{\partial z} + w\frac{\partial T'}{\partial z} = -w\left(\gamma_d + \frac{\partial T_e}{\partial z}\right) - k_5 T' \qquad \text{(iv)}$$

Multiply by g/T_e, average between $z = 0$ and $z = H/2$, and neglect the difference between the temperature and the virtual temperature. Then

$$\frac{\partial a}{\partial t} = -\overline{wg\frac{\partial (T'/T_e)}{\partial z}} + \overline{wg\frac{T'}{T_e^2}\frac{\partial T'}{\partial z}} - \overline{wg\frac{1}{T_e}\left[\frac{\partial T_e}{\partial z} + \gamma_d\right]} - k_5 a \qquad \text{(v)}$$

The second term on the right is assumed small as it is second order in T', S_d is defined by

$$\frac{w_{\max}}{H} S_d = -g\overline{\frac{w}{T_e}\left(\frac{\partial T_e}{\partial z} + \gamma_d\right)} \qquad \text{(vi)}$$

and we make the rough assumption that

$$wg\frac{\partial (T'/T_e)}{\partial z} \sim \frac{w_{\max}}{H} a$$

Then

$$\frac{\partial a}{\partial t} = \frac{w_{\max}}{H}(-S_d - a) - k_5 a \qquad (9)$$

The case of moist convection is derived similarly, with γ_m (assumed constant) substituted for γ_d.

List of principal symbols

a cloud conversion threshold.

a acceleration identified with the thermal component of buoyancy (m/sec²).

AC cloud autoconversion function; see Table 1.

B total buoyancy $= a - k_8 \mathcal{L}$.

CC cloud collection (accretion) function; see Table 1.

D diameter of an updraft column.

EP precipitation evaporation function; see Table 1.

F_1 parameter proportional to the condensation rate (evaporation rate) in a rising (descending) air column; unity when the air column is cloudy at all altitudes.

G condensation function; see Table 1.

H assumed height of an updraft or downdraft column.

k_5 assumed mixing rate for heat, momentum, and water substance associated with mixing in the horizontal plane.

k_6 coefficient that converts the evaporation rate to a rate of buoyancy change $[k_6 \approx 0.1$ (m/sec²)/(g H_2O/m³)].

k_8 coefficient that converts condensed water to an equivalent buoyancy [$k_8 \approx 0.01$ (m/sec²)/(g/m³)].

$\mathcal{L}$ average density of condensate in the vertical column of depth H ($\mathcal{L} = \overline{M + m}$).

m when positive, the cloud content; when negative, the saturation deficit.

m_0 environmental moisture.

M precipitation content of air.

N_0 precipitation particle size-distribution parameter.

S_d average thermal buoyancy approached as a dry air column sinks without mixing with its environment.

S_m average thermal buoyancy approached as a moist air column rises without mixing with its environment.

t time coordinate.

u horizontal wind.

V fall speed of precipitation relative to the air.

w vertical wind.

z vertical coordinate.

γ_m moist adiabatic lapse rate, a negative quantity.

γ_d dry adiabatic lapse rate, a negative quantity.

ϱ air density.

REFERENCES

Browning, K. A. 1964. Airflow and precipitation trajectories within severe local storms which travel to the right of the winds. *J. Atmos. Sci. 21*, 634–639.

Brunt, D. 1926. The period of simple vertical oscillations in the atmosphere. *Quart. J. R. Met. Soc. 53*, 30–32.

Byers, H. R. & Braham, R. R. 1949. *The thunderstorm.* U.S. Government Printing Office, Washington, D.C.

Charba, J. & Sasaki, Y. 1968. Structure and movement of the severe thunderstorms of 3 April 1964 as revealed from radar and surface meso-network data analysis. *ESSA Technical Memorandum ERLTM-41*, National Severe Storms Laboratory, Norman, Oklahoma.

Das, P. 1964. Role of condensed water in the life cycles of a convective cloud. *J. Atmos. Sci. 21*, 404–418.

Fankhauser, J. C. 1971. Thunderstorm-environment interactions determined from aircraft and radar observations. *Mon. Wea. Rev. 99*, 171–192.

Flora, S. 1953. *Tornadoes of the United States*, pp. 56–57. University of Oklahoma Press, Norman, Oklahoma.

Frank, N. L., Moore, P. L. & Fisher, G. E. 1967. Summer shower distribution over the Florida Peninsula as deduced from digitized radar data. *J. Appl. Met. 6*, 309–316.

Fujita, T. & Grandoso, H. 1969. Split of thunderstorm into anticyclonic and cyclonic storms and their motion as determined from numerical model experiments. *J. Atmos. Sci. 25*, 416–439.

Haglund, G. T. 1969. A study of a severe local storm of 16 April 1967. *ESSA Technical Memorandum ERLTM-44*, National Severe Storms Laboratory, Norman, Oklahoma.

Hammond, G. R. 1967. Study of a left-moving thunderstorm of 23 April 1967. *ESSA Technical Memorandum ERLTM-31*, National Severe Storms Laboratory, Norman, Oklahoma.

Kessler, E. 1969. On the continuity of water substance in atmospheric circulations. *Met. Monographs 10*, No. 33, 84 pp.

Kuo, H. L. 1969. Motions of vortices and circulating cylinder in shear flow with friction. *J. Atmos. Sci. 26*, 390–398.

Ludlam, F. H. 1963. Severe local storms: A review. *Met. Monographs 5*, 1–30.

Newton, C. W. 1960. Hydrodynamic interactions with ambient wind field as a factor in cumulus development. *Cumulus dynamics* (ed. C. E. Anderson), pp. 135–143. Pergamon Press, New York.

Ogura, Y. & Takahashi, T. 1971. Numerical simulation of the life cycle of a thunderstorm cell. *Mon. Wea. Rev. 99*, 895–911.

Ogura, Y. 1972. Cumulus modeling and parameterization, Convection Series 72-1, Unpublished typescript of the Laboratory for Atmospheric Research, Univ. of Illinois, Urbana, Illinois. (*Reviews of Geophysics and Space Physics*, in press.)

Pao, Y.-H. & Goldburg, A. (eds.) 1969. *Clear air turbulence and its detection.* Plenum Press, New York.

Priestley, C. H. B. 1953. Buoyant motions in a turbulent environment. *Australian J. Phys. 6*, 279–290.

Rasmussen, E. 1971. Diurnal variation of summertime thunderstorm activity over the United States. *USAFETAC TN 71-4*, U.S. Air Force Environmental Technical Applications Center, Washington, D.C. 20333, 12 pp.

Richardson, L. F. 1920. The supply of energy from and to atmospheric eddies. *Proc. R. Soc. London*, Ser. *A 97*, 354–373.

Richardson, L. F. 1926. Atmospheric diffusion shown on a distance-neighbor graph. *Proc. R. Soc. London*, Ser. *A 110*, 709–737.

Scorer, R. S. & Ludlam, F. H. 1953. Bubble theory of penetrative convection. *Quart. J. R. Met. 79*, 94–103.

Simpson, J. & Wiggert, W. 1969. Models of precipitating cumulus towers. *Mon. Wea. Rev. 97*, 471–479.

Squires, P. & Turner, J. S. 1962. An entraining jet model for cumulonimbus updrafts. *Tellus 14*, 422–435.

Srivastava, R. C. 1967. A study of the effect of precipitation on cumulus dynamics. *J. Atmos. Sci. 24*, 36–45.

Syono, S. & Takeda, T. 1962. On the evaporation of raindrops in a subcloud layer. *J. Met. Soc. Japan 40*, 245–265.

Turner, J. S. 1963. The motion of buoyant elements in turbulent surroundings. *J. Fluid Mech. 16*, 1–16.

Warner, J. 1970. Steady state one-dimensional models of cumulus convection. *J. Atmos. Sci. 27*, 1035–1040.

Weinstein, A. I. 1970. A numerical model of cumulus dynamics and microphysics. *J. Atmos. Sci. 27*, 246–255.

МОДЕЛЬ ОСАДКОВ И ВЕРТИКАЛЬНЫХ ПОТОКОВ ВОЗДУХА

Численно моделируется нестационарная влажная колонная конвекция. При этом вариант работы Пристли 1953 г. по изучению конвекции сухих термиков в турбулентной среде комбинируется с рассмотрением Кесслера 1969 г. распределений воды в циркуляции атмосферы. Даются решения одновременных уравнений для вертикальной скорости, плавучести, облачности и концентрации осадков в столбе воздуха, движущегося под влиянием силы тяжести, из которого выпадает дождь и который постоянно обменивается теплом, количеством движения и влагой с окружающим воздухом. Поле скорости в модели зависит от параметров вертикального градиента температуры в окружающем воздухе, содержания влаги и размеров, и амплитуды начального возмущения. Модель допускает затухающие колебания Брента–Вяйсяля, колебания конденсации и устойчивые подъемы воздуха трех родов. Наблюдаются большие изменения при переходе от одного типа решений к другому, когда параметры задачи переходят свои критические значения. Подробно и в связи с микрофизическими процессами анализируются соотношения между периодическими изменениями и стационарными величинами концентрации конденсированной воды, скоростью осадков, плавучестью и вертикальными скоростями воздуха.

В данной модели горизонтальный размер и маплтиуда возмущений архимедовой силы должны превзойти определенные величины, чтобы при данной влажности окружающего воздуха и данном условно неустойчивом вертикальном градиенте температуры началась стационарная влажная конвекция. Это ведет к рассмотрению свойств пограничного слоя, относящихся к географической и суточной изменчивости гроз. Высказывается мысль, что сильная статистическая неустойчивость внутри пограничного слоя стремится подавить развитие грозы, поскольку неустойчивый слой не поддерживает развитие больших волновых возмущений, которые могут быть существенными для инициирования глубокой конвекции и поскольку мелкомасштабная конвекция, возбуждаемая сильной неустойчивостью пограничного слоя, приводит к диссипации части энергии, которая в противном случае оставалась бы доступной для глубокой конвекции. Ряд других свойств гроз находит свое правдоподобное объяснение в рамках данной теории. Предлагаются также некоторые дальнейшие исследования для оценки справедливости данной теории и ее улучшения.